Available online at www.sciencedirect.com
SCIENCE DIRECT®
Journal of Marine Systems 45 (2004) 75–90
JOURNAL OF MARINE SYSTEMS
www.elsevier.com/locate/jmarsys

Pacific Ocean forecasts

Guillermo Auad*, Arthur J. Miller, John O. Roads

Climate Research Division, Scripps Institution of Oceanography, UCSD-0224, 9500 Gillman Drive, La Jolla, CA 92093, USA

Abstract

A primitive equation Pacific Ocean model forced by wind stresses and heat fluxes is used to obtain uncoupled forecasts of sea surface temperature (SST), heat storage (upper 400 m), and surface currents. The forecasts are displayed in real-time on the web http://ecpc.ucsd.edu) and are compared against observations obtained from the Reynolds (SST) and Joint Environmental Data Analysis Center, JEDAC http://jedac.ucsd.edu), (0- to 400-m temperature) data sets. The resulting forecast skill, for both total and anomalous fields, are reasonably good given the simplicity of our methodology and the fact that feedback processes between ocean and atmosphere are absent. SST forecasts are equal and even superior to anomaly persistence forecasts in some regions during some seasons. Given this skill, which depends both on model performance and on quality and sampling density of the observations, we are beginning to develop various applications for these experimental forecasts.

Keywords: Pacific Ocean; Forecast; Sea surface temperature; Heat storage; Ocean model; Midlatitudes

1. Introduction

Large-scale, seasonal oceanic anomalies in the extratropical regions are generally controlled by anomalous atmospheric forcing (e.g., Frankignoul, 1985; Cayan, 1992; Miller and Roads, 1990). The accuracy of seasonal forecasts of the extratropical ocean therefore depends on atmospheric seasonal forecasts, which have some skill on seasonal timescales (e.g., Roads et al., 2001). However, because extratropical oceanic conditions are very persistent, dynamical or statistical forecast skill levels that are superior to anomaly persistence forecasts are often difficult to achieve even for short-term forecasting (e.g., Miller et al., 1995; Cornuelle et al., 2000; Landman and Mason, 2001).

Teleconnections from anomalous tropical conditions (e.g., Alexander, 1992; Lau and Nath, 1996) may be able to add some level of skill to forecasts of the extratropical oceanic forcing. Also, some oceanic variations may be controlled by processes that are established by ocean dynamics, such as currents resulting from intrinsic oceanic instability processes (e.g., Robinson, 1996) or to Rossby wave propagation (Schneider and Miller, 2001). These oceanic processes may have predictability timescales that are longer than those of the atmosphere. Subsurface processes related to thermocline depth and geostrophic currents, and their effects on SST (e.g., through re-emergence, (Alexander et al., 2001) or through advection (Leeuwenburgh and Stammer, 2001) may also be more predictable than surface conditions.

Presently there are several groups around the world engaged in real-time forecasting of large-scale and mesoscale extratropical oceanographic conditions. The National Oceanographic and Atmospheric Ad-

* Corresponding author. Tel.: +1-619-822-1564; fax: +1-619-534-8561.
E-mail address: gauad@ucsd.edu (G. Auad).

0924-7963/$ - see front matter © 2004 Elsevier B.V. All rights reserved.
doi:10.1016/j.jmarsys.2003.11.010

ministration (NOAA) Coastal Ocean Forecast System (http://www.chartmaker.ncd.noaa.gov/csdl/COFS/v32/cofs32.html; see Aikman et al., 1996) predicts northwestern Atlantic Ocean conditions 24 h in advance. The Naval Research Laboratory (NRL) Experimental Real-Time North Pacific Ocean Nowcast/Forecast System (http://www7320.nrlssc.navy.mil/npacnfs www/index.html; see Harding et al., 1999) predicts North Pacific Ocean conditions 72 h in advance. The Forecasting Ocean–Atmosphere Model (http://www.meto.govt.uk/sec5/OA/FOAM/FOAM.html) predicts global ocean conditions 5 days in advance (Bell et al., 2000). The Mediterranean Forecasting System Pilot Project predicts Mediterranean Sea conditions 10 days in advance (Pinardi et al., 2001) (http://www.cineca.it/mfspp).

The Experimental Climate Prediction Center (ECPC) at the Scripps Institution of Oceanography has embarked on an experimental project to develop a seasonal forecasting model of the large-scale (non-eddy-resolving) extratropical Pacific Ocean conditions. We are exploring the relative importance of oceanic initial conditions, atmospheric forcing forecast skill and dynamical evolution of the ocean on the forecasts. Seasonal forecasts, (e.g., Auad et al., 2001a), are made on a regular basis and are displayed in near real-time on the web (http://ecpc.ucsd.edu/ocean/). A summary of the forecast and skill levels is presented herein.

This work is motivated by the impact that forecasts may have for fisheries management and pollution abatement agencies (e.g., public or governmental organizations such as the Mineral Management Service of the Department of Interior). In particular, an important goal is to establish the impact that three different (tropical) conditions, i.e., El Niño, La Niña and normal conditions, have on the extratropical forecast skill. These three conditions were dominant at different times during the 1998–2002 5-year study period which we use in this article. We also aim to establish the model forecast skill for different seasons and locations in the North Pacific Ocean for different variables. These variables, e.g., SST, heat storage are very important indicators in climatic studies and commercial activities such as fishing.

Accurate predictions of upper-ocean currents, and sea surface temperature and thermohaline structure, would be useful to these groups and agencies. The fisheries industry, for instance, needs to know in advance the SST field in order to plan their fleet operation (e.g., fuel consumption, number of vessels to be used). Sardine habitat is known to be restricted within the 13 and 23 °C isotherms (Tim Baumgartner, personal communication, also, in preparation, 2003), so knowing their future locations with some accuracy is also important. Our model can also predict the large-scale component (seasonal and subseasonal) of the surface velocity field, which is a key ingredient if one wants to obtain an accurate representation of the total velocity field. This component can be either used as boundary condition in regional models or just added to the local currents at every available location. The total velocity fields are also useful in establishing the evolution of oil spills in the ocean. The Mineral Management Service (MMS) of the US Department of Interior has been using oceanic forecasts for that purpose.

Given the environmental and commercial relevance of the California Current system and of the Gulf of Alaska, these two areas will be studied in detail. In addition, both areas have a high sampling rate of observations as compared to other regions of the North Pacific ocean.

In Section 2, we describe our methodology, in Section 3 we present the forecast results, leaving Section 4 for summary and conclusions.

2. Forecasting methodology

Forecasts for the Pacific Ocean are generated by (a) making uncoupled global atmospheric model forecasts forced by persistent initial SST anomalies and then (b) using the anomalous surface flux fields from the atmospheric forecast to drive an uncoupled Pacific Ocean model. The details of this procedure are now outlined.

2.1. Atmospheric model

The atmospheric model is the global spectral model (GSM), described in detail by Roads et al. (2001). It is based upon the medium range forecast (MRF) model used at the National Centers for Environmental Prediction (NCEP) for making the four times daily global data assimilation system (GDAS) analysis and for making the long-range (6–14 day)

predictions. This GSM, which has undergone steady improvement for a number of years, became on January 10, 1995, the basic global model used for the NCEP/NCAR reanalysis (hereafter referred to as NCEPR; see Kalnay et al., 1996).

The GSM uses a primitive equation or hydrostatic system of virtual temperature, humidity, surface pressure, mass continuity, vorticity, and divergence prognostic equations on terrain following sigma (sigma is defined as the ratio of the ambient pressure to surface pressure) coordinates. Our particular version of the GSM uses spherical harmonics with a triangular truncation of T62 and 18 irregularly spaced vertical levels (L18T62). These levels are concentrated near the lower boundary and tropopause.

The physics package for the GSM includes longwave and shortwave radiation interactions between cloud and radiation, boundary layer processes, such as shallow clouds and convection, large-scale condensation, gravity wave drag, and enhanced topography. Vertical transfer throughout the troposphere, including the boundary layer, is related to eddy diffusion coefficients dependent upon a Richardson number dependent diffusion process. A key parameterization development for the GSM was the innovative land surface parameterization (see Pan, 1990) which includes two soils layers. Another key GSM development effort has been the cumulus convection parameterization, which currently uses a simplified Arakawa–Schubert parameterization (see Pan and Wu, 1995). It should be noted that a number of more recent improvements have been implemented in NCEP models, which may ultimately prove useful in increasing the forecast skill (see e.g., Hong and Leetma, 1999); Kanamitsu, personal communication).

The initial conditions for the GSM forecasts come from the NCEP Global Data Assimilation System (GDAS) operational analysis (L28T126), which are posted in a timely fashion at NCEP. These higher resolution analyses are then transformed to lower resolution initial conditions (18LT62) by linearly interpolating between vertical sigma levels, spectrally truncating the spectral components, and bilinearly interpolating the higher resolution surface grids to our lower resolution grids (and land mask). Ocean conditions must be specified during the course of a prediction. We change the SST climatological component continuously throughout the integration, and persist the initial SSTA throughout the forecast integration. The sea–ice distribution is only changed climatologically. Twelve-week GSM forecasts are made once a week. These 12-week forecasts are then archived into weekly averages, which are further averaged into 3 monthly (4-week) averages.

2.2. Ocean model

The primitive equation ocean model called OPYC (Ocean isoPYCnal model) was developed by Oberhuber (1993) and has been used to study monthly through decadal-scale ocean variations over the Pacific Basin (e.g., Miller et al., 1994; Auad et al., 1998a,b). An updated version of the model with higher resolution and a revised forcing scheme was used by Auad et al., 2001a to assess hindcast skill for different forcing data sets. This updated model was also used for the present forecasting experiments.

The model is constructed with 10 isopycnal layers (each with nearly constant potential density and time- and space-dependent thickness, temperature, and salinity) that are fully coupled to a bulk surface mixed-layer model. The grid extends from 119°E to 70°W and from 67.5°S to 66°N, with artificial periodic boundary conditions along the latitudes of the Antarctic Circumpolar Current. The resolution is 1.5° in the midlatitude open ocean, with zonal resolution gradually increased to 0.65° resolution within a 20° band around the equator. Although the model is not eddy resolving, equatorial instability waves occur spontaneously, and eddies occur in the west wind drift of the midlatitudes. We only seek to study large-scale patterns in the response and regard this intrinsic variability as noise. The semi-implicit time step is 0.75 days.

2.3. Forcing and initial conditions

The monthly mean seasonal cycle forcing was derived from various sources and was previously used by Miller et al. (1994) and Auad et al. (2001a). In particular, the wind stress was derived from a combination of monthly mean European Centre for Medium-Range Weather Forecasts (ECMWF) midlatitude fields and monthly mean Hellerman–Rosenstein tropical climatology. The monthly mean seasonal cycle

climatology of turbulent kinetic energy (TKE) input to the mixed layer was estimated from the same data sets (Oberhuber, 1993). The surface freshwater flux was represented as a combination of observed monthly mean rainfall (Legates and Willmott, 1992), evaporation computed by bulk formula, plus a relaxation to the annual mean Levitus salinity field over 30-day timescales. The monthly mean seasonal cycle climatology of total surface heat flux was computed during spin-up (with no anomalous forcing) by determining surface heat flux at each time step with bulk formulae that use evolving model SST with ECMWF-derived atmospheric fields (air temperature, humidity, cloudiness, etc.); the daily mean seasonal cycle of heat flux was then saved (averaged over the last 10 years of a 99-year spin-up) and subsequently used as specified forcing during the anomalously forced forecasts.

Anomalous forcing fields of monthly mean wind stress, total surface heat flux, and TKE were computed from the atmospheric forecasts based on a 5-year climatology defined over the period 1998–2002. Even though this time frame is somewhat short to obtain reliable statistics, it allows for a reasonable comparison. During this time, known events such as El Niño and La Niña were present and provided useful information, such as the impact of these phenomena on the forecast skill. These fields were added to the seasonal cycle forcing functions following Killworth (1996). Within a few degrees of the equator, the surface heat fluxes generally serve as a damping mechanism (Barnett et al., 1991); so, a physically motivated Newtonian damping was employed to damp SST anomalies to the model SST climatology over 1–4-month timescales (see

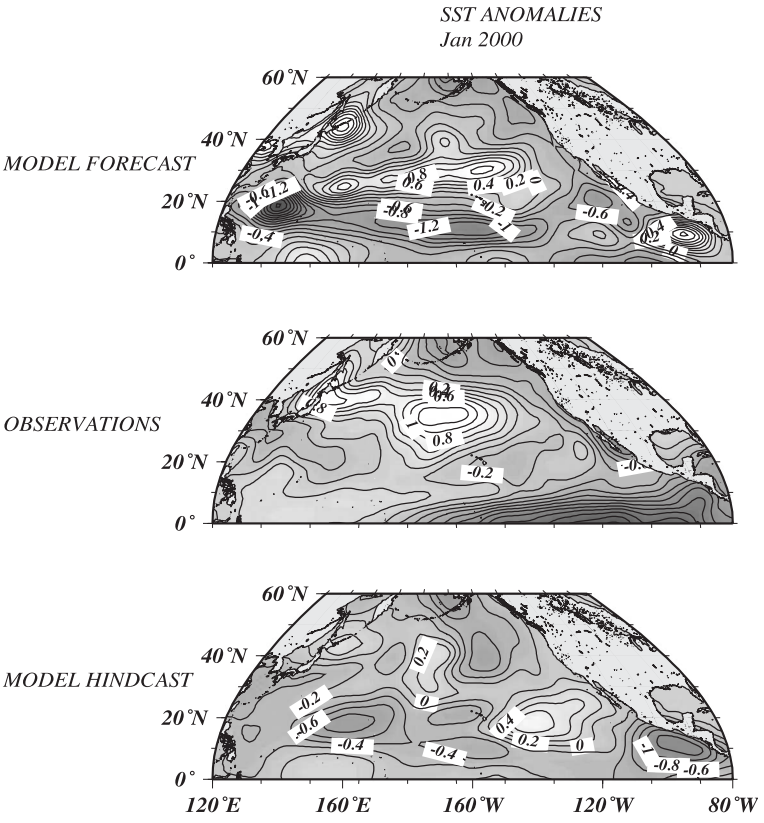

Fig. 1. Three-month lead forecast, hindcast and observations of sea surface temperatures (SST) for January of 2000. Contour interval (CI) is 0.2 °C. The hindcast run data is obtained by forcing the ocean model with NCEP/NCAR reanalysis wind stresses and heat fluxes from the previous month to the initial date. The forecast run then commences from that ocean state using wind stresses and heat fluxes forecast from the GSM. The observations come from the JEDAC data set.

Auad et al. (2001a) for a complete justification of this procedure).

The ocean model was initialized by an ocean hindcast driven up to the initial time by anomalous surface fluxes obtained from the NCEP/NCAR reanalysis and augmented with the operational analysis after September 26, 1997. This run was a continuation of the simulation discussed by Auad et al. (2001a).

Atmospheric predictions of wind stress and heat flux anomalies were then used to force the ocean model for one season (3 months). We chose this forecast timescale because it was long enough to allow the ocean to evolve from its (strongly persistent) initial state and yet short enough for the predicted atmospheric teleconnections from the tropics to be forced with reasonable accuracy by the persistent initial tropical oceanic conditions used in the atmospheric forecasts. After roughly 3 months, we expect that the coupling between the atmospheric boundary layer and the ocean surface layer will be too impor-

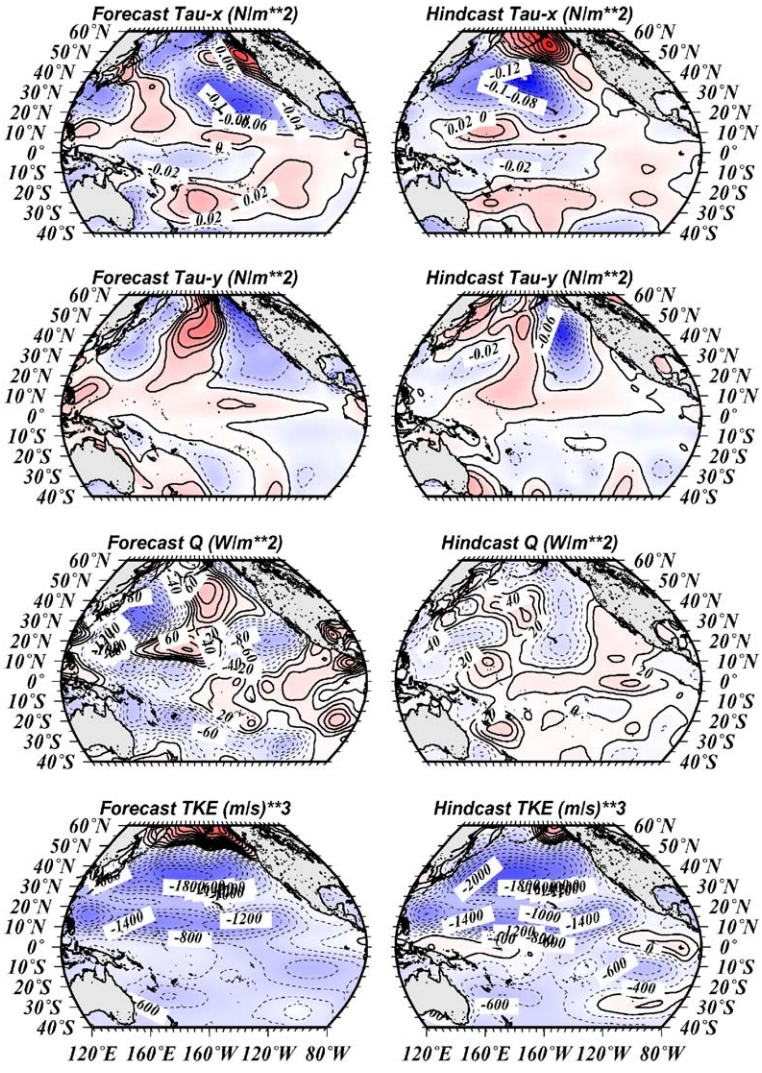

Fig. 2. Comparison between hindcast and 3-month forecast forcing functions, i.e., winds and heat fluxes and turbulent kinetic energy (TKE) for January of 2000. CI are, from top to bottom, 0.02 N m^2, 0.02 N m^2, 20 W m^2 and 200 m^3 s^{-3}.

tant to be ignored in the prediction of the surface fluxes.

Forecast products of sea surface temperatures (SST), heat storage of the upper 400 m of the ocean, thermocline depth, surface velocities, geostrophic surface velocities, mixed layer depth, temperatures from 0 to 400 m along the equator, wind stress and net surface heat fluxes, are posted on the ECPC web page (http://ecpc.ucsd.edu/ocean/) at the beginning of each month. As part of an automatized post processing routine, the anomalous oceanic fields are also estimated and then displayed on-line along with total fields.

2.4. Skill assessment

Forecast skill was quantitatively assessed using a weighted measure of rms error defined as

$$S = 1.0 - \frac{D}{V} \tag{1}$$

where

$$D = (y_o - y_f)^2$$

and V is the variance of the observations, while y_o and y_f are the observed and forecast variables,

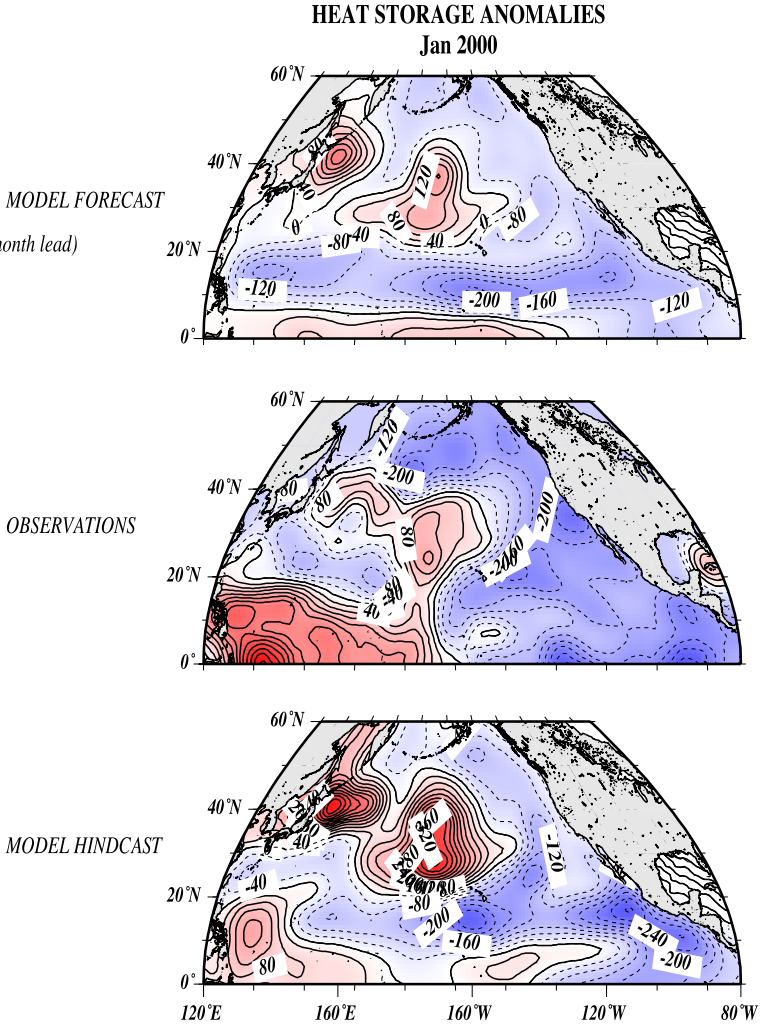

Fig. 3. As in Fig. 1 but for heat storage of the upper 400 m. CI is 40 × 10^8 J m^{-2}.

respectively. The second measure of the skill, is simply a measure of the error variance relative to the total observed anomaly variance averaged over a region or averaged over an ensemble of forecasts. For Eq. (1), observed and forecast anomalies were defined with respect to climatologies from 1998 to 2002. Heat storage and SST observations are from the Joint Environmental Data Analysis Center (JEDAC) (http://jedac.ucsd.edu) and Reynolds (ftp://podaac.jpl.nasa.gov) data sets, respectively.

3. Forecast results

3.1. Three-month lead forecast

We now discuss a typical Pacific Ocean forecast, using January 2000 as a representative verification state. Fig. 1 shows the SST anomaly for a 3-month lead forecast for January, 2000, along with the corresponding ocean model hindcast (using analysis instead of GSM forecasts to drive the ocean model)

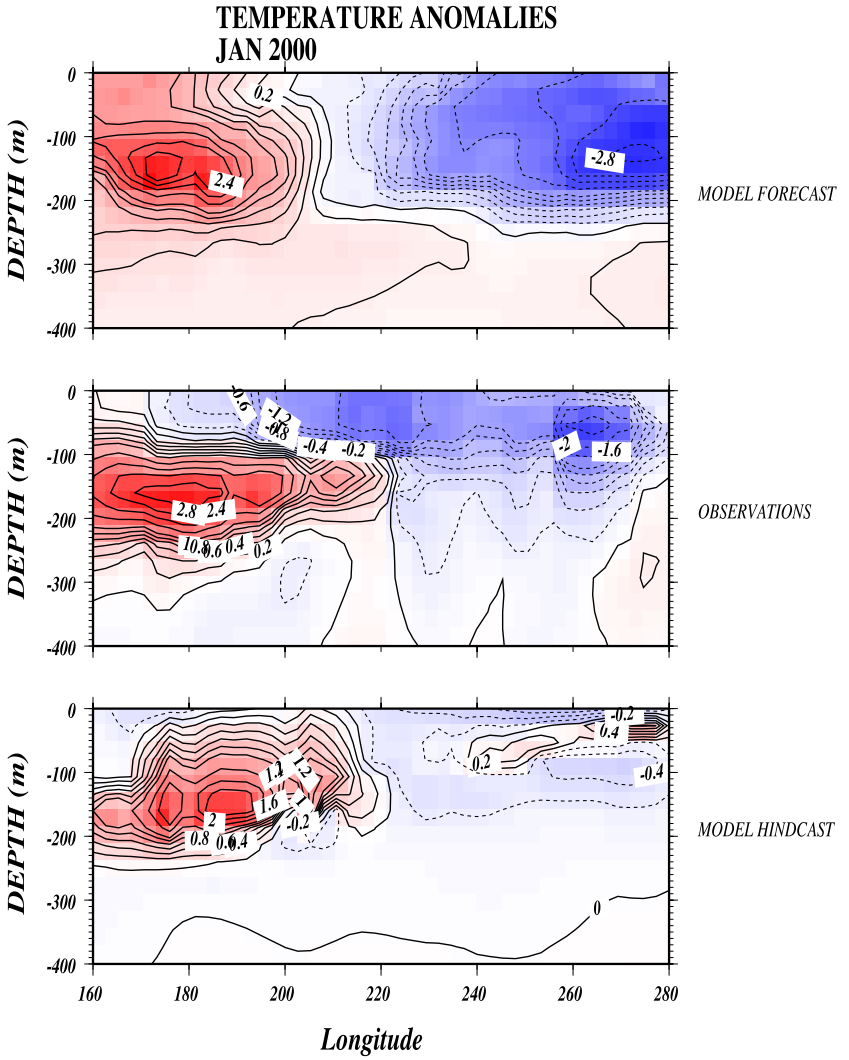

Fig. 4. As in Fig. 1 but for temperature along the equator. CI is 0.2 °C.

and available ocean observations. A general feature of all three panels is the positive SST anomaly seen in the central North Pacific, in the region near Japan and in the western equatorial Pacific, and cold regions in the Gulf of Alaska and in the western subtropical North Pacific around 20°N. The amplitude varies considerably among the three plots. The differences between top and bottom panel are due to differences in the forcing functions between both runs. The size of the differences between hindcast and forecast is similar to those between forecast and observations. The visual correspondence among SST forecast, observations and hindcast for other winter months is comparable to that of Fig. 1 and is quantified below.

A comparison of the hindcast and forecast anomalous forcing functions for January 2000 (Fig. 2) reveals the different anomalous wind stress and heat fluxes in areas where the hindcast and forecast SSTs are in disagreement (e.g., in the eastern subtropical gyre region). Most egregious are the discrepancies between the surface heat fluxes which have an immediate impact on SST. Errors in wind stress affect Ekman current advection which concurrently affects

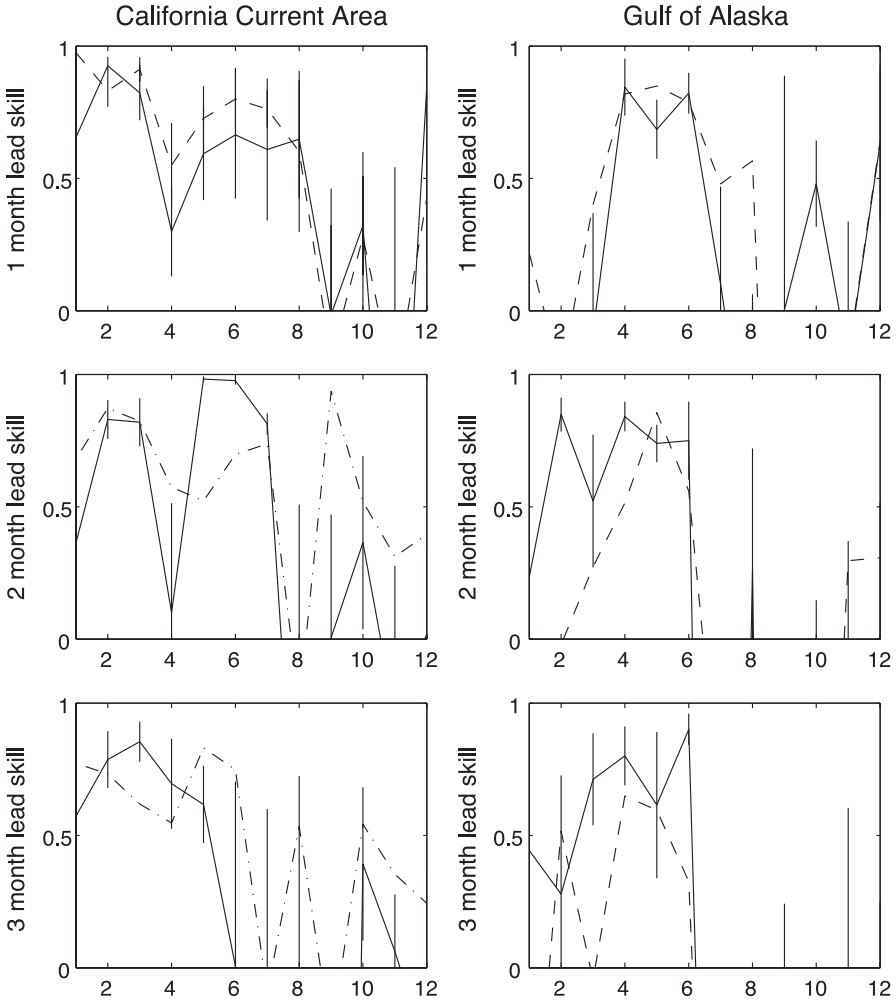

Fig. 5. From top to bottom, 1-, 2- and 3-month lead rms model (solid line) and persistence (dashed lines) skill of the zonal wind stress averaged for the California Current System (CCS), left column, and the Gulf of Alaska (GAL), right column. The error bars represent the standard deviation of the plotted skills over the 1998–2002 period.

SST and geostrophic current advection, which can have a lagged response on SST.

Heat storage is affected not only by the state of the SST but also by the state of the thermocline, which has a forced component due to wind stress curl and heating and a dynamic component due to wave propagation and advection (Auad et al., 1998a,b). Deeper in the water column, the relative in influence of direct atmospheric forcing decreases and the in influence of ocean dynamics increases. Fig. 3 shows the 3-month lead forecast, observations and hindcast maps for heat storages of the upper 400 m for January 2000. The predicted heat storage fields are qualitatively superior to the predicted SST fields, with differences between forecast and hindcast heat storages being of similar magnitude to those between forecast and observed heat storages.

Fig. 4 shows equatorial vertical profiles of forecast, observed and hindcast temperature. These figures highlight the superior skill found in the subsurface fields. They also indicate the model can forecast some aspects of tropical ocean variations without coupled ocean–atmosphere dynamics. However, in this article, the tropical strip should be

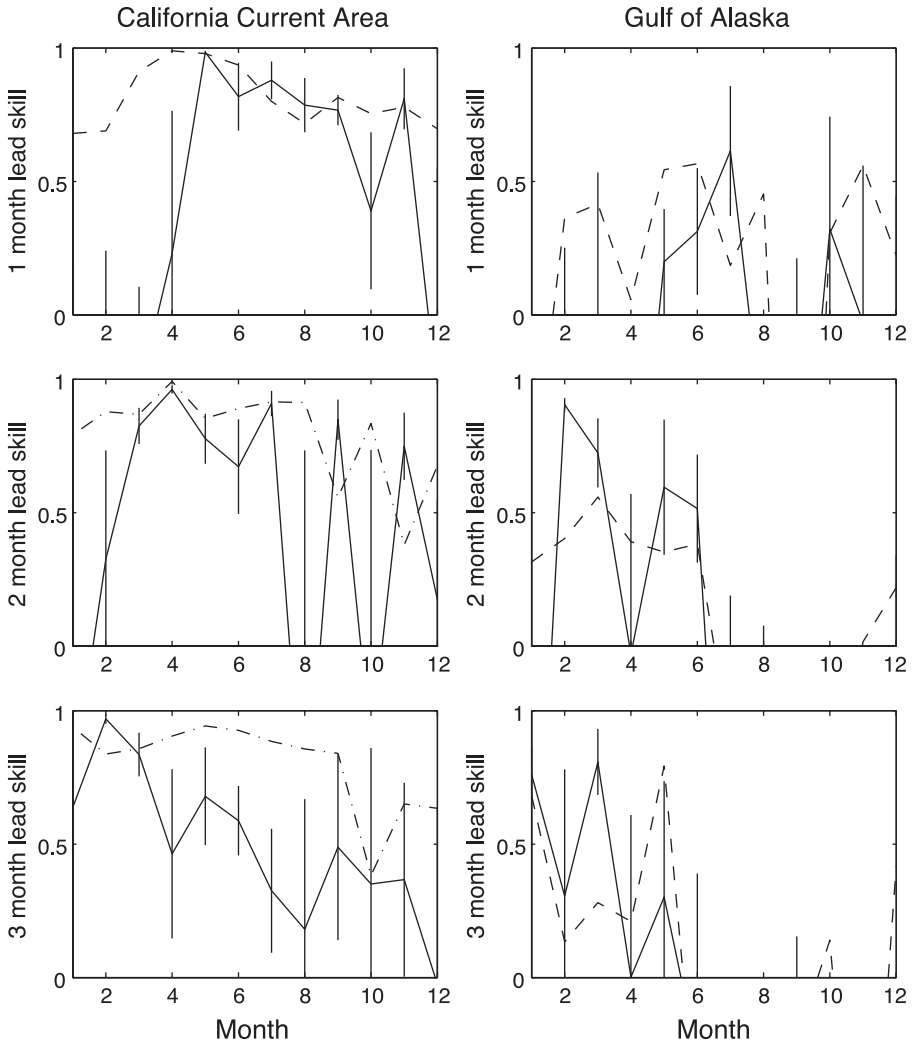

Fig. 6. As in Fig. 5 but for surface net heat fluxes.

regarded as a natural boundary condition since our focus is currently on the midlatitudinal North Pacific ocean.

3.2. Quantification of the forecast skill

3.2.1. Atmospheric forcing

In this section, we quantify the model skill by estimating Eq. (1) in two key areas of the eastern North Pacific ocean: the Gulf of Alaska (GAL: 168°W–130°W, 46°N–58°N)) and the California Current System (CCS: 130°W-coast, 34°N–58°N). The variable in question is averaged over these areas and then Eq. (1) is evaluated for every month and year. The resulting skills and standard deviations, as error bars, will be shown as monthly averages taken from the 5-year long records. In the estimation of these bars, there are included one post El Niño year (1998), one La Niña year (1999), two normal conditions years (2000–2001), and one pre El Niño year (2002). Thus, we

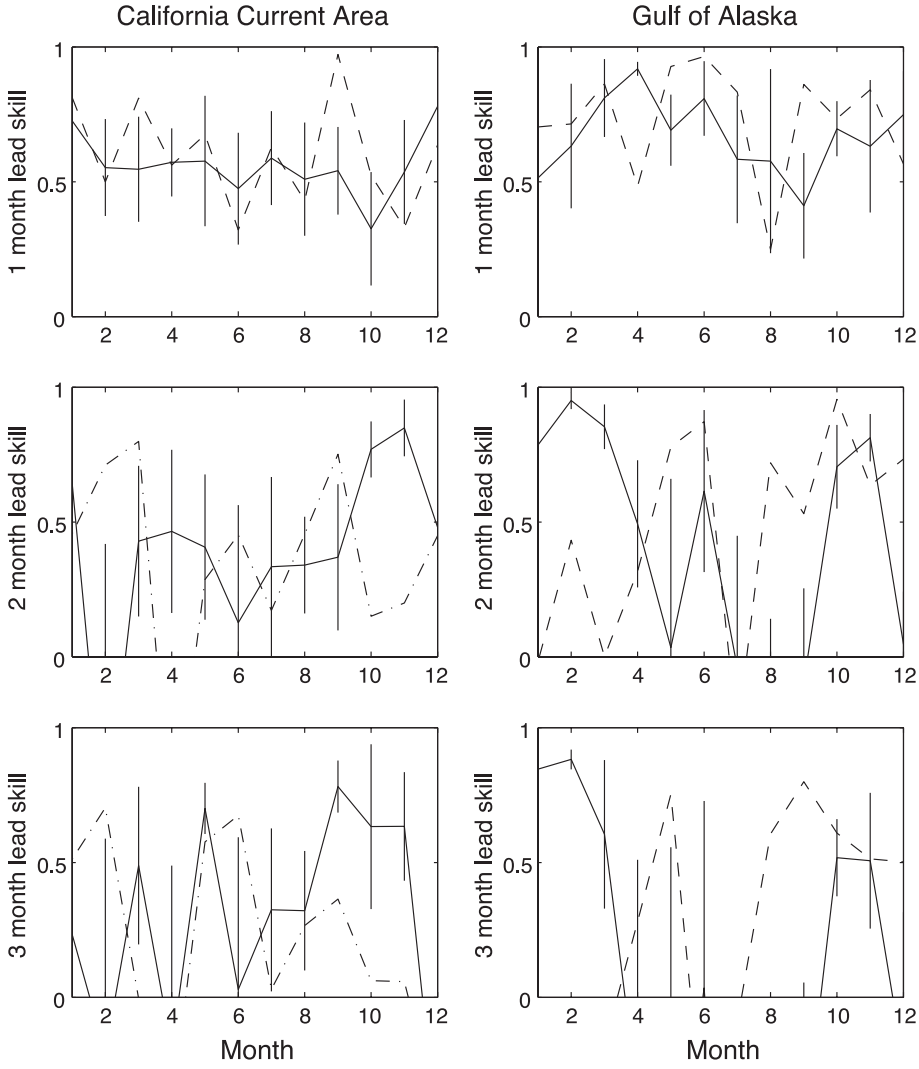

Fig. 7. From top to bottom, 1-, 2- and 3-month lead rms model (solid line) and persistence (dashed lines) skills of SST averaged for the California Current System (CCS), left column, and the Gulf of Alaska (GAL), right column.

consider our 5-year long time series to be fairly balanced in terms of processes of interannual variability.

Fig. 5 shows the zonal wind stress forecast and persistence (from model hindcast) for the GAL and CCS areas. The CCS (left column) shows the highest model and persistence skills for winter (February and March) and Spring (April, May and June). The Summer and Fall seasons are less skilled for both model and persistence, while a similar description applies for the GAL area (right column). In both areas, the model beats persistence for at least one season for time leads longer than 1 month. However, some of the model and persistence skill estimates overlap (e.g., 1-month lead in august and for the CCS area). Those months for which the curves take negative values, as defined by Eq. (1), are not shown.

It is important to note that the difference between model and persistence skills increases with time lead for January, March, April, May and June in the GAL. For surface heat fluxes, Fig. 6, the CCS area persistence skill is seldom beat by the model skill which drops down with increasing time lead for spring, summer and fall and rises up with increasing time lead for winter. The build up of model skill with time lead for winter is likely due to the combination of poor initial conditions with sustained realistic boundary forcing. The GAL (Fig. 6, right column) has a smaller persistence skill than the CCS, and seems to owe most of its model skill to boundary forcing. The model beats persistence in February and March for 2- and 3-month lead times and in May and June for 2-month time lead.

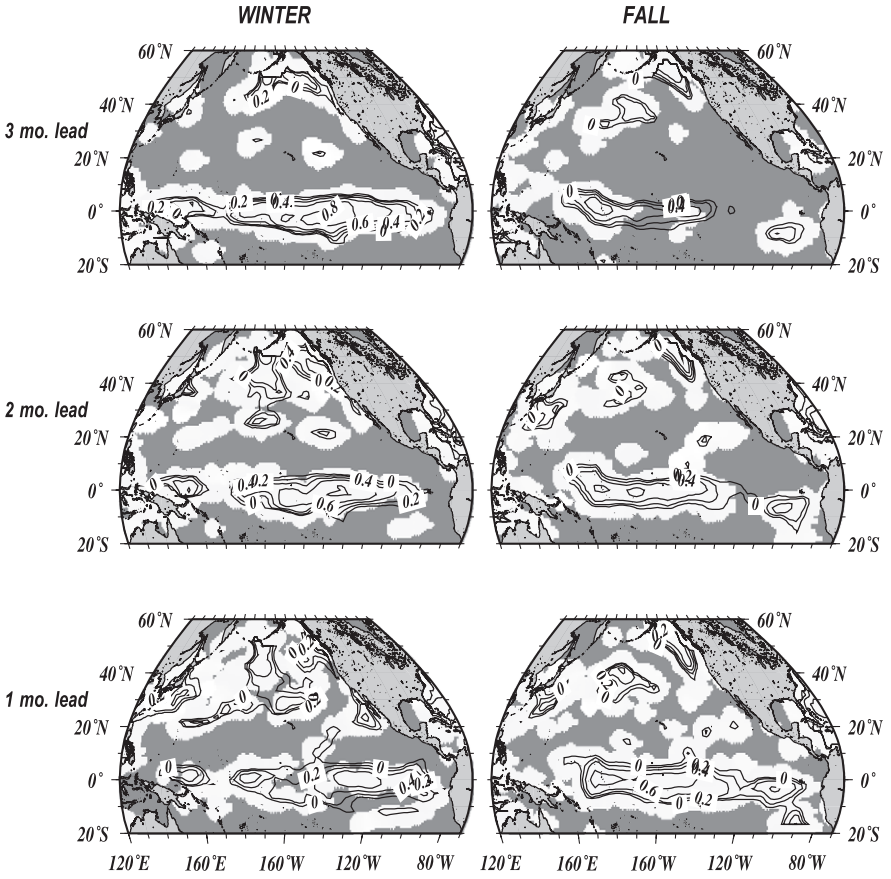

Fig. 8. SST RMS skill for winter (left column) and fall (right column). From top to bottom the 3-, 2- and 1-month lead forecast are shown. Contours are only drawn when the model rms skill is greater than zero, while the white shaded areas correspond to areas where the model skill beats that one of persistence. Contour interval is 0.2.

3.2.2. SST

The oceanic response to the atmospheric forecasts is described for the SST and heat storage fields. In the CCS area, the model skill for SST (Fig. 7, left column) decreases with time lead in winter, spring and summer, but builds in fall. This build up leads to a reasonable model predictability during the fall season for 2- and 3-month lead times. This predictability is enhanced by the notorious decay of the persistence skill, during the fall season of the SST persistence skill. Helped by the sudden drop of the persistence skill from the 1- to the 2-month lead time in the GAL area (Fig. 7, right column), the ocean model yields the highest skills in the winter season (JFM) for 2- and 3-month time leads. The only month, for 1-month lead time, in which the model outperforms persistence is April, and this is likely due to appropriate initial conditions at the end of March. After then, for 2- and 3-month lead times, likely due to errors in the forcing functions, the model skill significantly drops below persistence. The fact that the model skill dramatically decreases from the first to the last lead time, and between April and September, points out to the need of improving the quality of the atmospheric

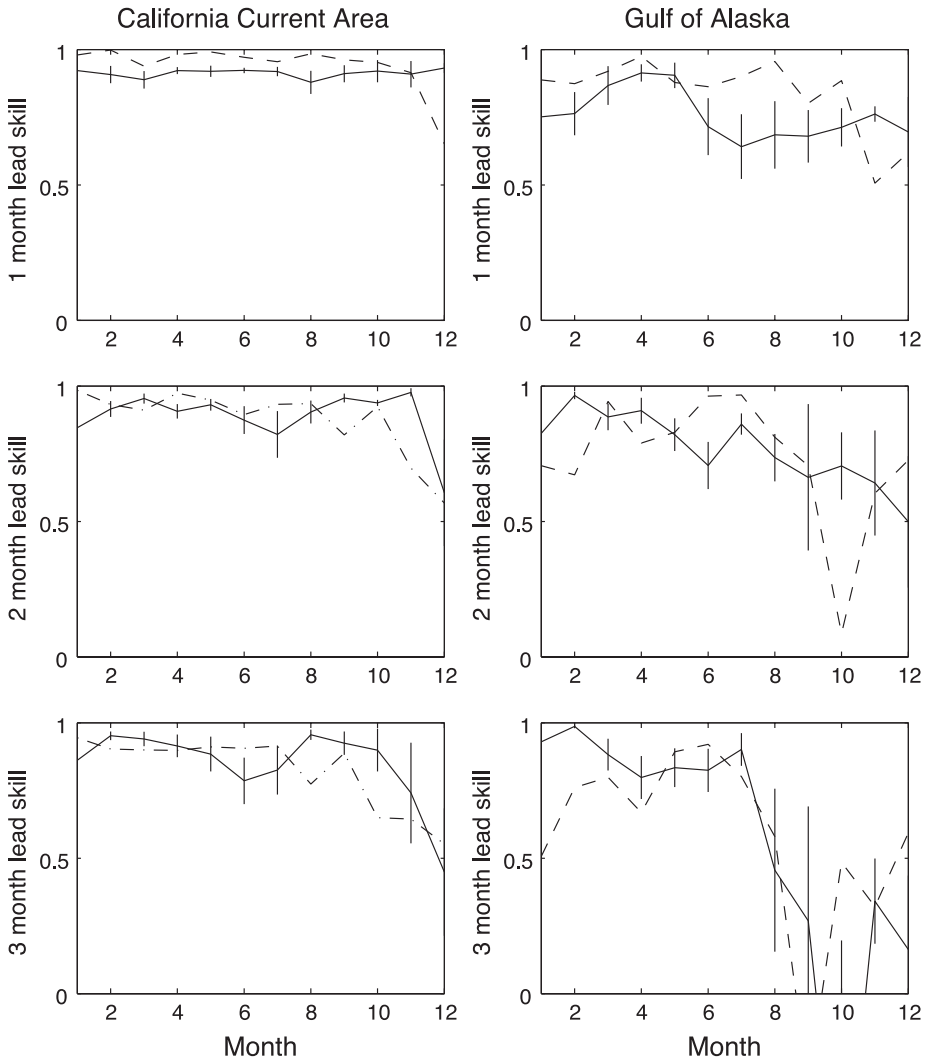

Fig. 9. As in Fig. 7 but for heat storage.

forecasts in the GAL area, particularly during spring and summer.

The spatial structure of the dynamic model forecast skill score (Eq. (1)) is shown in Fig. 8 for winter and fall. Also shown is the difference in skill between dynamic and anomaly persistence forecasts (unshaded regions indicate dynamic superiority). Midlatitude regions north of 20°N tend to be more skillfully forecast than those of the subtropical North Pacific where persistence forecasts are superior. The structure of high skill is reminiscent of the canonical midlatitude SST structure seen in typical statistical pattern analyses at seasonal through decadal timescales (Tanimoto et al., 1993). Large regions of the tropics are also skillful and superior to persistence at longer leads for both winter and fall. The model is not skillful in midlatitudes during the spring and summer months (not shown). The seasonal differentiation emerges as a result of the larger signal to noise ratios induced by the stronger winds of the fall and winter seasons. After the spring transition, late April–early May in the northern hemisphere, the weak wind signal is more easily masked in the background noise of the model internal dynamics. Minor changes were obtained when the last 2 years, of all time series involved in the estimation of the maps of Fig. 8, were eliminated.

3.2.3. Heat storage (0–400 m)

Model and persistence skill for heat storage are higher than those for SST since its temporal and spatial changes have a slower evolution. In general

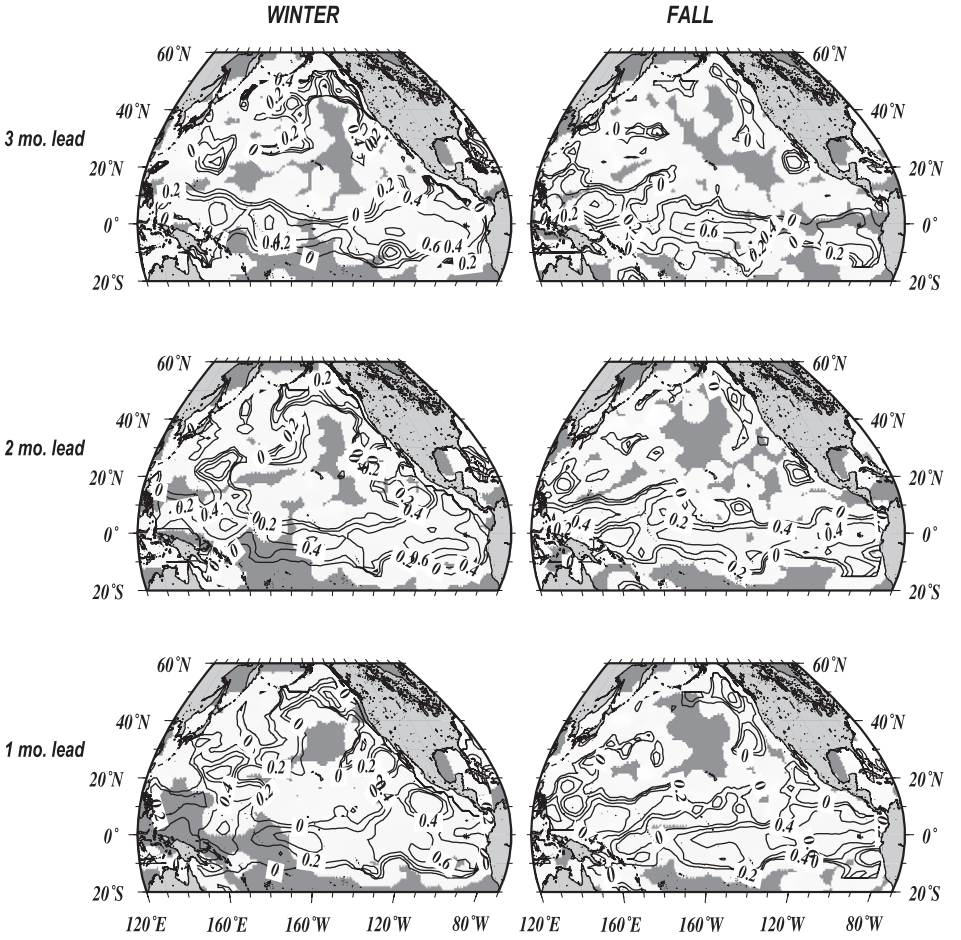

Fig. 10. As in Fig. 8 but for heat storage.

terms, during the fall and winter seasons persistence skill in the CCS area drops faster, with lead time, than model skill (Fig. 9, left column). In summer, the opposite situation takes place and this could be related to either poor atmospheric forecasts or simply to the fact that in the CCS area, the summer winds are much weaker than in fall/winter; i.e., the model skill will be mostly dependent on initial conditions. A similar situation to that one just described for fall in the CCS takes place for winter in the GAL area. Both areas also have in common that model skill beat persistence skill for the last 2 month of the year for the 1-month lead time. Unlike SSTs, heat storages have higher model skills in the summer months, which tend to confirm the already mentioned dependence of the SST field on the seasonality of the atmospheric functions. On the other hand, heat storage is more dependent, than SST, on the ocean dynamics and which makes it more sensitive to the quality of the initial conditions than SST.

The spatial structure of the skill defined by Eq. (1) for winter heat storage forecasts is shown in Fig. 10. The other seasons are not shown because unlike SST, heat storage is less affected by the seasonality felt at the air–sea interface. For instance, in the central North Pacific, forecast skill is higher in spring than in winter, unlike SSTs. Forecast heat storage skill shows almost no seasonality at all in the California Current region with year-round skill of about 0.5–0.6. In these two areas, the model has been shown to successfully mimic the observations in terms of interannual Rossby wave activity (Auad et al., 1998a). The 3-month lead heat storage forecast skill, for the winter, spring and summer seasons, reaches 0.70 in the western tropical Pacific which is comparable to more sophisticated models of the tropical ocean for the same time lead (Ji et al., 1998).

4. Discussion and conclusion

The experimental ocean forecasts shown in this article constitute a first step toward a more accurate and complete large-scale Pacific Ocean forecasting system. Generating higher skill levels at the longer lead times, for these and other physical variables, is our immediate goal while providing useful forecasts for various applications, is our ultimate goal.

The present results were highlighted by forecasts of anomalous SST that are superior to persistence forecasts in some regions of the extratropical Pacific Ocean for lead times of up to 3 months in the winter and fall seasons. The forecasts of anomalous heat storages had similar skill levels relative to persistence but a less marked difference between seasons due to the inclusion of deeper data in the computation of heat storages. Although dynamic forecasts of tropical variables do not include tropical ocean–atmosphere interactions, the short-lead forecast skill levels, there are comparable to those of more sophisticated models. As an example, the model was able to forecast the mild warming of the eastern tropical Pacific for 2001 (Auad et al., 2001b) as well as the occurrence of an eastward propagating equatorial Kelvin wave (Auad et al., 2001c) that was later identified in Topex-Poseidon imagery (The ENSO signal, http://www.esig.ucar.edu/signal, issue 18, August 2001).

The OPYC SST and heat storage forecasts are particularly useful in the California Current system and Gulf of Alaska areas. The fact that the model beats persistence in fall and winter, for both variables and for all time leads, is probably related to the more accurate representation of the model forcing functions there, and in the neighboring California Current System area where the sampling of observations is higher than in other areas. The model winter and fall SST also beat persistence and for all time leads in the central North Pacific and in the Kuroshio Oyashio Extension. For heat storage, instead, the central North Pacific region can be forecast with greater skill than persistence, in both fall and winter and for all three time leads.

Errors in (a) the estimation of the forcing functions, (b) the determination of the initial conditions, (c) model physics approximations and resolution and (d) sampling errors in the observations, contribute to ocean model forecast error. At this stage of forecast model development, errors due to model initial conditions dominate the forecasts in the first month and errors in estimated forcing functions dominate in months two and three. Ocean data assimilation would improve the oceanic initial states and our future research is aimed toward the development of an appropriate initial state.

The incorporation of atmospheric–oceanic feedbacks, through the coupling of oceanic and atmospheric models, could lead to an increased forecast

skill especially for the tropics but potentially also for the northwestern Pacific Ocean as well (Schneider and Miller, 2001). The forecast model skill, for both SST and heat storage, along 40°N, near the Kuroshio–Oyashio Extension (KOE), beats persistence for winter and fall, and for all time leads with the exception of the 3-month winter estimation, for both SSTs and heat storages and for all seasons. However, a large area south of around 40°N is not accurately forecast by OPYC, probably because air–sea feedbacks were neglected here (see Schneider et al., 2002). The KOE mean path and mean amplitude are, however, well represented in the model. Predictability of the KOE might also depend on the thermocline initial conditions, which could affect the overlying SSTs (Deser et al., 1996; Miller et al., 1998; Xie et al., 2000). The KOE is a key area in climatic research as it has recently been found (Schneider et al., 2002) that it drives the overlying atmosphere through the damping of SST anomalies during the winter season. However, it is still an open question if this damping is timescale dependent. Auad (in preparation 2003) suggests that winter decadal damping (i.e., the damping that takes place on decadal timescales when one considers winter anomalies only) is preferred over other decadal seasons or to any season in the interdecadal band. The absence of explicit feedbacks in the ocean model is therefore not a major shortcoming if one focuses on extratropical and seasonal variability.

Finally, the ocean model provides forecasts of subsurface variables in regions where there are virtually no subsurface observations available. Even though the anomaly model forecast skill in these regions is uncertain, it can at least be estimated by comparison of the ocean model forecast and hindcast (driven by NCEP reanalysis forcings). This knowledge is currently being applied to the development of forecast products which can be readily exploited by fisheries management and pollution abatement, among other applications. In this respect, it is our goal to eventually implement a fisheries outlook for the eastern Pacific Ocean. Working alongside marine biologists and biological oceanographers, we could, for instance, forecast the physical boundaries that contain most of the sardine population off the California coasts. Sardines, like other marine species, have habitats and/or reproductive phases (e.g., spawning) regulated by environmental conditions.

Acknowledgements

This paper was funded by the National Oceanic and Atmospheric Administration, Office of Global Programs, under Grants NA17R1231 and NA47GP0188. The views expressed herein are those of the authors and do not necessarily reflect the views of NOAA. We thank Warren White for providing us with the temperature data of the JEDAC center. We also thank Mr. Jack Ritchie for his efforts to routinely run our experimental forecasts in near real-time.

References

Aikman III, F., Mellor, G.L., Ezer, T., Sheinin, D., Chen, P., Breaker, L., Bosley, K., Rao, D.B., 1996. Towards an operational nowcast/forecast system for the U.S. East Coast. In: Malanotte-Rizzoli, P. (Ed.), Modern Approaches to Data Assimilation in Ocean Modeling, Elsevier Oceanography Series, vol. 61. Elsevier, Amsterdam, pp. 347–376.

Alexander, M.A., 1992. Midlatitude atmosphere ocean interaction during El Niño: 1. The north Pacific-Ocean. J. Climate 9, 944–958.

Alexander, M.A., Timlin, M.S., Scott, J.D., 2001. Winter-to-winter recurrence of sea surface temperature, salinity and mixed layer depth anomalies. Prog. Oceanogr. 49, 41–61.

Auad, G., Miller, A.J., White, W.B., 1998a. Simulation of heat storages and associated heat budgets in the pacific ocean: 1. El Niño-southern oscillation timescale, J. Geophys. Res. 103, 27,603–27,620.

Auad, G., Miller, A.J., White, W.B., 1998b. Simulation of heat storages and associated heat budgets in the Pacific Ocean: 2. Interdecadal timescale, J. Geophys. Res. 103, 27, 621–27,635.

Auad, G., Miller, A.J., Roads, J.O., Cayan, D.R., 2001a. Pacific Ocean wind stresses and surface heat fluxes from the NCEP Reanalysis and observations: cross-statistics and ocean model responses, Journal of Geophysical Research 106, 22,249–22,265.

Auad, G., Miller, A. J., Roads, J. O., Ritchie, J., 2001b. Seasonal Forecasts of the Tropical and Extratropical Pacific Ocean: MAM 2001 Forecast. Experimental Long Lead Forecast Bulletin, March issue.

Auad, G., Miller, A.J., Roads, J.O., Ritchie, J., 2001c. Seasonal forecasts of the extratropical Pacific Ocean: JJA forecast. Experimental Long Lead Forecast Bulletin, June issue. COLA (Institute of Global Environment and Society), Calverton, Maryland 20705, USA.

Barnett, T.P., Latif, M., Kirk, E., Roeckner, E., 1991. On ENSO physics. J. Clim. 4, 487–515.

Bell, M.J., Forbes, M.R., Hines, A., 2000. Assessment of the FOAM global data assimilation system for real-time operational ocean forecasting. J. Mar. Syst. 25, 1–22.

Cayan, D.R., 1992. Latent and sensible heat flux anomalies over the

northern oceans: driving the sea surface temperature. J. Phys. Oceanogr. 22, 859–881.

Cornuelle, B.D., Chereskin, T., Niiler, P.P., et al., 2000. Observations and modeling of a California undercurrent eddy. J. Geophys. Res.-Oceans 105, 1227–1243.

Deser, C., Alexander, M.A., Timlin, M.S., 1996. Upper ocean thermal variations in the North Pacific during 1970–1991. J. Climate 9, 1840–1855.

Frankignoul, C., 1985. Sea-surface temperature anomalies, planetary-waves, and air–sea feedback in the middle latitudes. Rev. Geophys. 23, 357–390.

Harding, J., Carnes, M., Preller, M.C., et al., 1999. The naval research laboratory role in naval ocean prediction. Mar. Technol. Soc. J. 33, 67–79.

Hong, S.Y., Leetma, A., 1999. An evaluation of the NCEP RSM for regional climate modeling. J. Climate 12, 592–609.

Ji, M., Behringer, D.W., Leetmaa, A., 1998. An Improved Coupled Model for ENSO Prediction and Implications for Ocean Initialization: Part II. The coupled model. Mon. Weather Rev. 126, 1022–1034.

Kalnay, E., et al., 1996. The NMC/NCAR reanalysis project. Bull. Am. Meteorol. Soc. 4, 437–471.

Killworth, P., 1996. Time interpolation of forcing fields in ocean models. J. Phys. Oceanogr. 4, 136–143.

Landman, W.A., Mason, S.J., 2001. Forecasts of near-global sea surface temperatures using canonical correlation analysis. J. Climate 14, 3819–3833.

Lau, N.C., Nath, M.J., 1996. The role of the "atmospheric bridge" in linking tropical Pacific ENSO events to extratropical SST anomalies. J. Climate 9, 2036–2057.

Leeuwenburgh, O., Stammer, D., 2001. The effect of ocean currents on sea surface temperature anomalies. J. Phys. Oceanogr. 31, 2340–2358.

Legates, D.R., Willmott, C.J., 1992. A comparison of GCM-simulated and observed mean January and July precipitation. Glob. Planet. Change 97, 345–363.

Miller, A.J., Roads, J.O., 1990. A simplified coupled model of extended-range predictability. J. Climate 3, 523–542.

Miller, A.J., Cayan, D.R., Barnett, T.P., Graham, N.E., Oberhuber, J.M., 1994. Interdecadal variability of the Pacific Ocean: model response to observed heat flux and wind stress anomalies. Clim. Dyn. 9, 287–302.

Miller, A.J., Poulain, P., Robinson, A.R., Arango, H.A., Leslie, W.G., Warn-Varnas, A., 1995. Quantitative skill of quasigeostrophic forecasts of a baroclinically unstable Iceland-Faroe Front. J. Geophys. Res. 100, 10,833–10,849.

Miller, A.J., Cayan, D.R., White, W.B., 1998. A westward-intensified decadal change in the North Pacific thermocline and gyre-scale circulation. J. Climate 11, 3112–3127.

Oberhuber, J.M., 1993. Simulation of the Atlantic circulation with a coupled sea ice-mixed layer isopycnal general circulation model: Part I. Model description. J. Phys. Oceanogr. 22, 808–829.

Pan, H.L., 1990. A simple parameterization scheme of evapotranspiration over land for the NMC medium-range forecast model. Mon. Weather Rev. 118, 2500–2512.

Pan, H.L., Wu, W.S., 1995. Implementing a mass flux convective parameterization package for the NMC medium-range forecast model. NMC Office Note, vol. 409. NCEP/NMC, Camp Springs, Maryland 20746, USA, 40 pp. [Available from NCEP/EMC, 5200 Auth Road Camp Springs MD 20746].

Pinardi, N., Demirov, E., Tonani, M., 2001. Mediterranean Forecasting System Pilot Project: the initial forecasting phase. EuroGOOS Space Panel (Font, J., Gaspar, P., Guymer, T. H., Johannessen, J., Van der Kolff, G. H., Le Provost, C., Ratier, A., Williams, D., Flemming, N. C.), EuroGOOS Conference on Operational Ocean Observations from Space. EuroGOOS Publication No. 16 Southampton Oceanography Centre Southampton ISBN 0-904175-44-8.

Roads, J.O., Chen, S.C., Fujioka, F., 2001. ECPC's weekly to seasonal global forecasts. Bull. Am. Meteorol. Soc. 82, 639–658.

Robinson, A.R., 1996. Physical processes field estimation and an approach to interdisciplinary ocean modeling. Earth-Sci Rev. 40, 3–54.

Schneider, N., Miller, A.J., 2001. Predicting western North Pacific Ocean climate. J. Climate (letters) 14, 3997–4002.

Schneider, N., Miller, A.J., Pierce, D.W., 2002. Anatomy of North Pacific decadal variability. J. Climate 15, 586–605.

Tanimoto, Y., Iwasaka, N., Hanawa, K., Toba, Y., 1993. Characteristic variations of sea surface temperature with multiple timescales in the North Pacific. J. Climate 6, 1153–1160.

Xie, S.P., Kunitani, T., Kubokawa, A., Nonaka, M., Hosoda, S., 2000. Interdecadal thermocline variability in the North Pacific for 1958–1997: a GCM simulation. J. Phys. Oceanogr. 30, 2798–2813.